



## RFDR with adiabatic inversion pulses: Application to internuclear distance measurements

Jörg Leppert, Oliver Ohlenschläger, Matthias Görlach & Ramadurai Ramachandran\*

Abteilung Molekulare Biophysik/NMR-Spektroskopie, Institut für Molekulare Biotechnologie, 07745 Jena, Germany

Received 11 June 2003; Accepted 6 October 2003

**Key words:** adiabatic pulse, internuclear distance, solid state NMR, RFDR

### Abstract

In the context of the structural characterisation of biomolecular systems via MAS solid state NMR, the potential utility of homonuclear dipolar recoupling with adiabatic inversion pulses has been assessed via numerical simulations and experimental measurements. The results obtained suggest that it is possible to obtain reliable estimates of internuclear distances via an analysis of the initial cross-peak intensity buildup curves generated from two-dimensional adiabatic inversion pulse driven longitudinal magnetisation exchange experiments.

With the introduction of a variety of dipolar recoupling sequences (Bennett et al., 1994; Griffin, 1998; Dusold and Sebald, 2000), it is now possible to obtain resonance assignments, to measure distances and torsion angles and to undertake structural characterisation of isotopically labelled biological systems via MAS solid state NMR. In fact, the first MAS NMR derived structure of a protein, namely the SH3 domain of  $\alpha$ -spectrin, has been reported recently by Castellani et al. (2002). Employing biosynthetically site-directed labelled samples the structure of the protein was obtained from a set of approximate distance restraints derived from Proton Driven Spin Diffusion (PDS) experiments (Szeverenyi et al., 1982). For minimising the heat dissipated in the probe by the RF irradiations employed it is advantageous to employ the PDS technique in internuclear distance measurements. However, as mentioned by Castellani et al. (2002) and others (Sun et al., 1997; Hong, 1999), quantitative evaluation of PDS cross-peak intensities in terms of internuclear distances is difficult. The PDS approach is also inefficient in the sense that very large mixing times on the order of hundreds of milliseconds are typically required to obtain measurable cross-peak intensities (Hong, 1999). For structure elucidation it will be preferable to employ methods

that are more efficient and conveniently amenable for quantitative analysis.

Broadband dipolar recoupling sequences can be employed to extract multiple distance constraints from site selectively  $^{13}\text{C}$ -enriched samples. However, many of the dipolar recoupling sequences such as POST C7 (Hohwy et al., 1998), CMR7 (Rienstra et al., 1998) and DRAWS (Gregory et al., 1995) employ CW irradiation with rotor-synchronised RF phase alternations to recouple homonuclear dipolar interactions. The RF field strength required in such sequences is a multiple  $N$  of the spinning speed employed. For example, typical  $N$  values used with POST C7, CMR7 and DRAWS are 7, 7 and 8.5, respectively. Unlike resonance assignment studies, the measurement of long range distances between low  $\gamma$  nuclei could involve the application of dipolar recoupling sequences over a period of 10–30 ms. CW irradiation coupled with large RF field strength required for efficient implementation of many of the dipolar recoupling sequences might result in sample heating problems. One way to minimise sample heating problems is to measure distances between high  $\gamma$  nuclei such as  $^1\text{H}$ . This has been demonstrated recently by Reif et al. (2003) with ( $^2\text{H}$ ,  $^{15}\text{N}$ )-labelled samples of the  $\alpha$ -spectrin SH3 domain. Alternatively, for distance measurements involving low  $\gamma$  nuclei dipolar recoupling sequences that would lead to minimal sample heating effects can be employed. In this context it is appealing to use the

\*To whom correspondence should be addressed. E-mail: raman@imb-jena.de

RFDR (Bennett et al., 1992, 1998) sequence as it involves the application of only one  $180^\circ$  pulse per rotor period.

RFDR is a zero-quantum recoupling sequence that has found application for obtaining two-dimensional longitudinal magnetisation exchange spectra. With short dipolar recoupling times, only spins in spatial proximity lead to cross peaks of appreciable intensities thereby facilitating assignment of  $^{13}\text{C}$  resonances in uniformly labelled peptides/proteins (McDermott et al., 2000; Pauli et al., 2000). Two-dimensional RFDR with longitudinal magnetisation exchange has also been successfully applied earlier for internuclear distance measurements (Griffiths et al., 1994; Zaborowski et al., 1999; Gilchrist et al., 2001). One of the main difficulties with the conventional RFDR sequence, however, is that if the chemical shift separation between the recoupled nuclei is small, e.g., for amide  $^{15}\text{N}$  nuclei of the peptide backbone and aliphatic side chain  $^{13}\text{C}$  resonances, the dipolar recoupling efficacy is reduced considerably. Under very fast magic angle spinning conditions this problem can be overcome via the fpRFDR technique (Ishii, 2001). Very high spinning speeds, however, may be difficult to employ with some systems, for example to avoid sample dehydration. In this context, we have shown recently that it is advantageous to employ RFDR with adiabatic inversion pulses for obtaining  $^{13}\text{C}$  chemical shift correlation spectra of uniformly labelled peptides/proteins at moderate MAS frequencies (Heise et al., 2002; Leppert et al., 2003). Even for distance measurements involving nuclei with small chemical shift anisotropy and where spinning sideband intensities will not be significant, moderate MAS frequencies could be sufficient. Therefore, we have assessed via numerical simulation and  $^{15}\text{N}$  RFDR experimental measurements the potential of Adiabatic Inversion pulse Driven Magnetisation Exchange (AIDME) experiments for obtaining distance constraints. The results from these investigations are encouraging and are presented below.

Numerical simulations were carried out using the SIMPSON program (Bak et al., 2000) considering two spin-1/2  $^{15}\text{N}$  nuclei, a Zeeman field strength of 11.7 T, typical  $^{15}\text{N}$  chemical shift parameters and a spinning speed of 7 kHz. The adiabatic inversion pulses ‘cagauss’ (Kupce and Freeman, 1996; Leppert et al., 2003) with 142  $\mu\text{s}$  duration,  $\omega_1(\text{max})/2\pi$  of  $\sim 22$  kHz and a frequency sweep width of 40 kHz, as implemented in the Varian pulse shaping software ‘Pbox’, were employed. Besides the p5d  $\{0^\circ, 240^\circ,$

$240^\circ, 60^\circ, 0^\circ\}$  adiabatic pulse phasing scheme (Tycko et al., 1985), the m4 supercycle (Levitt et al., 1983) was also employed for better preservation of longitudinal magnetisations at longer mixing times.  $^{15}\text{N}$  RFDR experiments with one pulse per rotor period were performed with undiluted  $^{15}\text{N}$  and  $\{^{15}\text{N}, ^{13}\text{C}\}$  labelled samples of uracil and histidine, respectively, at room temperature on a 500 MHz wide bore Varian UNITY INOVA solid state NMR spectrometer equipped with a 5 mm DOTY supersonic triple resonance probe and a waveform generator for pulse shaping. Cross-polarisation under Hartmann–Hahn matching conditions was employed and all spectra, unless mentioned otherwise, were collected under high power  $^1\text{H}$  decoupling ( $\sim 90$  kHz). Typical  $^1\text{H}$  and  $^{15}\text{N}$   $90^\circ$  pulse widths were 2.8 and 7.5  $\mu\text{s}$ , respectively. Other details are given in the figure captions.

The results obtained from numerical simulations are given in Figure 1. In these simulations, as in our earlier study (Leppert et al., 2003), we have monitored as a function of the dipolar mixing time, the magnitude of longitudinal magnetisation transferred to spin 2 starting with  $z$  magnetisation on spin 1 at zero recoupling time. Figure 1A shows that even with the long adiabatic pulse employed, the initial rate of transfer of magnetisation from spin 1 to spin 2 is highly sensitive to the dipolar coupling strength and hence to internuclear distances. As shown in Figure 1B, dipolar recoupling with adiabatic pulses is more efficient than with rectangular pulses. It is worth noting that while the inversion bandwidth of adiabatic pulses can be tailored as per the experimental requirements, with rectangular pulses the inversion bandwidth only gets reduced with increasing pulse length. As the extraction of distance constraints from cross-peak intensity buildup curves would get considerably simplified, it would be advantageous if the efficacy of dipolar recoupling is not significantly influenced by the isotropic and anisotropic chemical shift parameters, relative CS tensor orientation and by the orientation of the internuclear dipolar vector. To assess the performance of AIDME, simulations were carried out for different dipolar coupling strengths and with typical values of  $^{15}\text{N}$  isotropic and anisotropic chemical shift parameters. The efficacy of dipolar recoupling with adiabatic inversion pulses is not very much affected by the chemical shift parameters (Figures 1C and 1D). Typically, the initial buildup rates are faster when the isotropic chemical shift difference is smaller and when there is no CSA. The chemical shift and dipolar tensor orientational parameters also

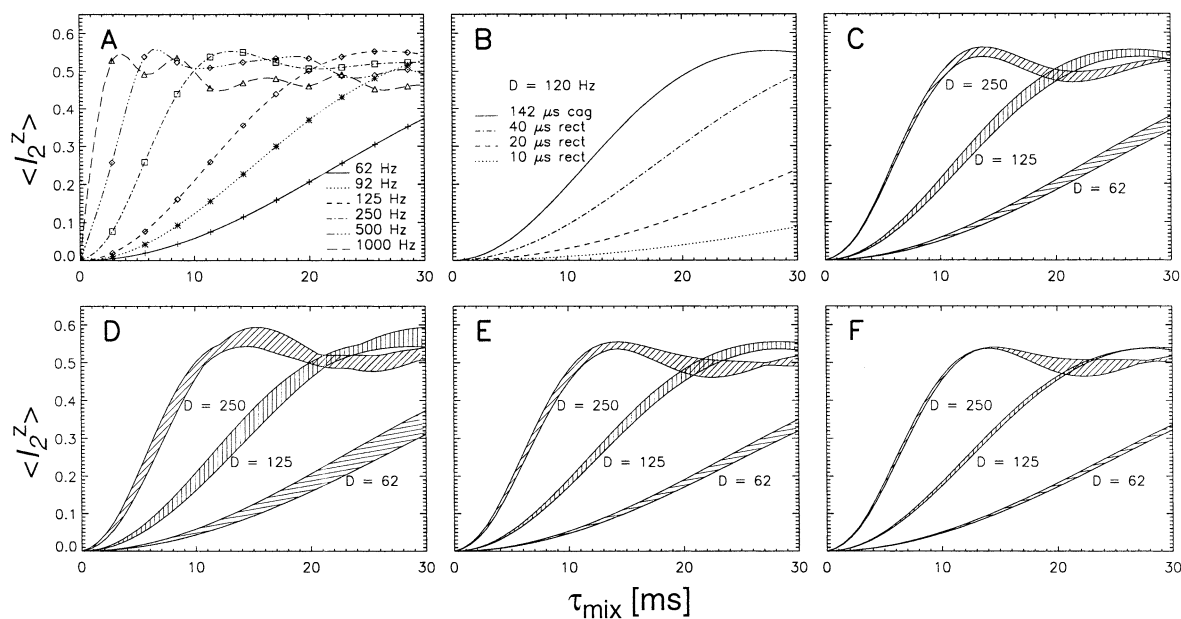


**Figure 1.** Simulated adiabatic inversion pulse driven longitudinal magnetisation transfer characteristics. The plots show the magnitude of the transferred magnetisation (normalised to the maximum transferable signal) at the second nitrogen spin starting with  $z$  magnetisation on spin 1 at zero recoupling time. Simulations were carried out at a spinning speed of 7000 Hz, with ‘cagauss’ adiabatic pulses (142  $\mu\text{s}$ , 22.0 kHz  $\gamma H_1$ ) employing the [p5d m4] phasing scheme (see text) and in time increments of 20 rotor periods. The resulting data points were interpolated to provide visual clarity. The plots show the dependence of the initial rate of buildup on the (A) dipolar coupling strength, (B) type of inversion pulse employed, (C) isotropic chemical shift differences, (D) magnitude of chemical shift anisotropy, (E) relative orientation of the CS tensors and (F) orientation of the dipolar tensor. All simulations were carried out keeping the RF carrier on resonance with spin 1. The plots A-C were generated neglecting CSAs. The different dipolar coupling strengths employed are indicated in the simulated plots. Simulations shown in A and B were carried out employing a value of 900 Hz for the isotropic chemical shift difference ( $\Delta\delta$ ) between the recoupled nuclei. In B the simulated plots with rectangular inversion pulses of different durations were generated employing the xy-8 (Gullion et al., 1990) phasing scheme. The shaded areas in C-F represent the initial buildup rates observed over the range of the parameter mentioned. Simulations C-F were generated considering the following chemical shift and other parameters: (C)  $\Delta\delta = 50 \dots 2500$  Hz, (D)  $\Delta\delta = 900$  Hz,  $\delta_{\text{aniso}}(\text{N1,N2}) = -62.8 \dots 97.5$  ppm,  $\eta = 0.179 \dots 0.9$ , the Euler angles defining the relative orientation of CS tensors  $\Omega_{1,2}$  were fixed at  $(0^\circ, 0^\circ, 0^\circ)$  and the orientation of the dipolar vector in the CS tensor frame of spin N1 is fixed at  $(0^\circ, 0^\circ)$ , (E)  $\Delta\delta = 1500$  Hz,  $\delta_{\text{aniso}}(\text{N1}) = 97.5$  ppm,  $\eta(\text{N1}) = 0.179$ ,  $\delta_{\text{aniso}}(\text{N2}) = 66.7$  ppm,  $\eta(\text{N2}) = 0.9$ , the Euler angles  $\Omega_{1,2}$  was chosen in all combinations  $0^\circ$  and  $90^\circ$ , (F)  $\Omega_{1,2}$  was fixed at  $(0^\circ, 0^\circ, 0^\circ)$ , other chemical shift parameter values employed were as in Figure E and the orientation of the dipolar vector in the CS tensor frame of spin N1 varied as  $(0^\circ, 0^\circ)$ ,  $(0^\circ, 90^\circ)$  and  $(90^\circ, 0^\circ)$ .

do not significantly influence the recoupling dynamics (Figures 1E and 1F). This is in contrast to what is observed with rectangular inversion pulses (data not shown). In short, it should be feasible to obtain reliable estimates of internuclear distances via AIDME spectroscopy. The experimental results presented below confirm these expectations.

$^{15}\text{N}$ - $^{15}\text{N}$  dipolar recoupling experiments were carried out on polycrystalline samples of  $^{15}\text{N}$  and ( $^{15}\text{N}$ ,  $^{13}\text{C}$ )-labelled uracil and histidine, model systems employed recently in our MAS NMR investigations (Heise et al., 2002; Leppert et al., 2000). These represent systems with different chemical shift parameters and presumably also different chemical shift and dipolar tensor orientational parameters. Figure 2 shows experimental results obtained from 2D PDS and

AIDME experiments. Spectral cross-sections taken at the N1 site are shown in Figure 2 as a function of the dipolar mixing time. A representative 2D spectrum from each experiment is also shown in Figure 2. The  $^{15}\text{N1}$ - $^{15}\text{N3}$  dipolar coupling in the systems investigated is in the range of 100 Hz ( $\sim 116$  Hz (2.2 Å) for histidine and  $\sim 100$  Hz (2.3 Å) for uracil) and the experimental cross-peak intensity buildups are essentially consistent with the simulations shown in Figure 1. In contrast to PDS, AIDME can lead to cross-peaks with substantial intensities even with short dipolar mixing times (Figure 2). Figure 3 shows representative plots of experimental normalised centerband cross-peak intensities together with simulated curves computed with different  $^{15}\text{N}$ - $^{15}\text{N}$  distances as a function of the dipolar mixing time. From the data

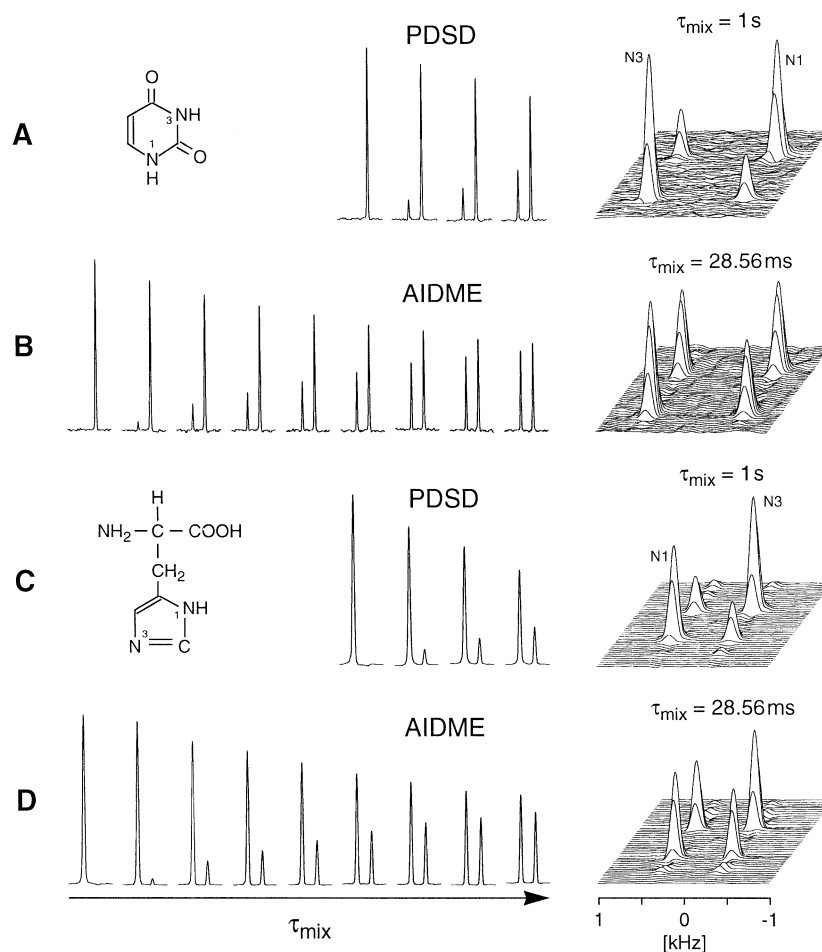


**Figure 2.** Experimental spectral data (zoomed plots) of uracil (A, B) and histidine (C, D) obtained from 2D PDS and AIDME experiments. Spectral cross-sections taken at the N1 sites are shown as a function of the dipolar mixing time. The mixing times employed in the PDS and AIDME experiments were (0.0, 0.25, 0.5 and 1 s) and (0.0, 5.71, 11.43, 14.29, 17.14, 20.0, 22.85, 25.71 and 28.56 ms) respectively. A representative 2D spectrum from each experiment at the mixing time indicated is also given. The data for uracil and histidine were collected employing a spinning speed of 7000 Hz, recycle times of 16 s and 8 s, 16 scans per  $t_1$  increment,  $\omega_1$  spectral widths of 3000 Hz and 6000 Hz and with 32 and 64  $t_1$  increments, respectively. The AIDME spectra were collected employing ‘cagauss’ adiabatic inversion pulses of 142  $\mu$ s duration,  $\omega_1(\text{max})/2\pi$  of  $\sim 22$  kHz, frequency sweep width of 40 kHz, with the [p5d m4] pulse phasing scheme (see text) and keeping the RF carrier at the center of the  $^{15}\text{N}1$  and  $^{15}\text{N}3$  resonances.

given in Figure 3 it is seen that reliable estimates of internuclear distances can be obtained. As we were only interested in assessing the possibilities for obtaining approximate, but reliable, internuclear distance constraints, only the isotropic chemical shifts that can be easily obtained in general have been considered in the simulated plots shown in Figure 3. The effects of chemical shift anisotropy, chemical shift and dipolar tensor orientations and relaxation effects were neglected. Inclusion of these, where possible, together with sample dilution, measurements at low temperature and other precautions can further improve the accuracy of the distance constraints generated. For

example, even if the magnitude of the CS tensor principal values could not be measured exactly in the system under investigation, incorporation of typical CSA values taken from model systems could lead to better distance constraints. This has been also observed for the systems studied here (data not shown).

Similar to the  $^{15}\text{N}$ - $^{15}\text{N}$  distance measurements demonstrated here, adiabatic inversion pulse driven magnetisation exchange spectroscopy can also be effectively employed for  $^{13}\text{C}$ - $^{13}\text{C}$  internuclear distance measurements even in situations where the isotropic chemical shift difference between the recoupled nuclei is small. As already mentioned earlier, it is possible

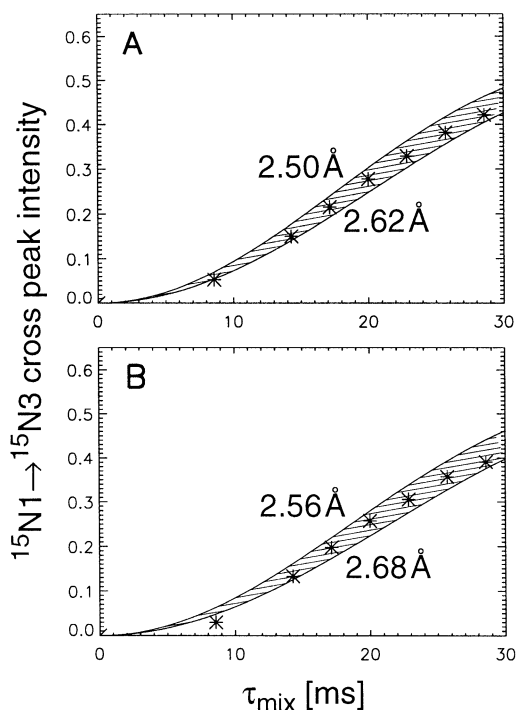


Figure 3. Experimental  $^{15}\text{N1} \rightarrow ^{15}\text{N3}$  AIDME centerband cross-peak intensity buildup in uracil (A) and histidine (B). The experimental cross-peak intensities were normalised to the measured  $^{15}\text{N1}$  diagonal peak intensity at zero mixing time. Figures 3A and 3B also show the expected initial rate of buildup of cross-peak intensities (shaded area) for  $^{15}\text{N}$ - $^{15}\text{N}$  internuclear distances in the range indicated. Simulated plots were generated employing the isotropic chemical shifts of the two  $^{15}\text{N}$  nuclei in the systems under investigation.

to tailor the adiabatic pulse characteristics (such as the frequency sweep width and duration) to obtain the desired bandwidth of excitation employing only the minimum required RF field strength. This will aid in reducing not only sample heating arising from the recoupling RF field but also help in minimising the interference between the decoupling and recoupling RF fields. Although till date only a few reports involving  $^{15}\text{N}$ - $^{15}\text{N}$  dipolar recoupling have been published in the literature (Weintraub et al., 1994a, b), the quality of data presented in Figure 2 suggests that it is possible to employ conveniently  $^{15}\text{N}$ - $^{15}\text{N}$  dipolar recoupling experiments in the study of biological systems. For example, as the distances between amide nitrogen sites on adjacent residues in helical regions in peptides/ proteins are in the range of only 2.75–2.95 Å ( $\sim 60$ –50 Hz), dipolar recoupling experiments can be employed for the identification of helical regions in a peptide/protein.  $^{15}\text{N}$ - $^{15}\text{N}$  dipolar recoupling experi-

ments would also be useful in the study of RNAs and such studies are in progress.

## References

- Bak, M., Rasmussen, J.T. and Nielsen, N.C. (2000) *J. Magn. Reson.* **147**, 296–330.
- Bennett, A.E., Griffin, R.G. and Vega, S. (1994) *NMR Basic Principles and Progress*, Springer Verlag, Berlin, **33**, 1–77.
- Bennett, A.E., Ok, J.H., Griffin, R.G. and Vega, S. (1992) *J. Chem. Phys.*, **96**, 8624–8627.
- Bennett, A.E., Rienstra, C.M., Griffiths, J.M., Zhen, W., Lansbury, P.T. and Griffin, R.G. (1998) *J. Chem. Phys.*, **108**, 9463–9479.
- Castellani, F., van Rossum, B., Diehl, A., Schubert, M., Rehbein, K., and Oschkinat, H. (2002) *Nature*, **420**, 98–102.
- Dusold, S. and Sebal, A. (2000) *Annu. Rep. NMR Spectrosc.*, **41**, 185–264.
- Gilchrist, Jr., M.L., Monde, K., Tomita, Y., Iwashita, T., Nakanishi, K. and McDermott, A.E. (2001) *J. Magn. Reson.*, **152**, 1–6.
- Gregory, D.M., Mitchell, D., Stringer, J.A., Kihne, S.R., Shiels, J.C., Callahan, J., Mehta, M.A. and Drobny, G.P. (1995) *Chem. Phys. Lett.*, **246**, 654–663.
- Griffin, R.G. (1998) *Nat. Struct. Biol.*, **5**, 508–512.
- Griffiths, J.M., Lakshmi, K.V., Bennett, A.E., Raap, J., van der Wielen, C.M., Lugtenburg, J., Herzfeld, J. and Griffin, R.G. (1994) *J. Am. Chem. Soc.*, **116**, 10178–10181.
- Gullion, T., Baker, D.B. and Schaefer, J. (1990) *J. Magn. Reson.*, **89**, 479–484.
- Heise, B., Leppert, J., Ohlenschläger, O., Görlach, M. and Ramachandran, R. (2002) *J. Biomol. NMR*, **24**, 237–243.
- Hohwy, M., Jakobsen, H.J., Eden, M., Levitt, M.H. and Nielsen, N.C. (1998) *J. Chem. Phys.*, **108**, 2686–2694.
- Hong, M. (1999) *J. Biomol. NMR*, **15**, 1–14.
- Ishii, Y. (2001) *J. Chem. Phys.*, **114**, 8473–8483.
- Kupce, J. and Freeman, R. (1996) *J. Magn. Reson. A*, **118**, 299–303.
- Leppert, J., Heise, B., Ohlenschläger, O., Görlach, M. and Ramachandran, R. (2003) *J. Biomol. NMR*, **26**, 13–24.
- Leppert, J., Heise, B. and Ramachandran, R. (2000) *J. Magn. Reson.*, **145**, 307–314.
- Levitt, M.H., Freeman, R. and Frenkiel, T. (1983) *Adv. Magn. Reson.*, **11**, 47–110.
- McDermott, A., Polenova, T., Bockmann, A., Zilm, K.W., Paulsen, E.K., Martin, R.W. and Montelione, G.T. (2000) *J. Biomol. NMR*, **16**, 209–219.
- Pauli, J., von Rossum, B., Förster, H., de Groot, H.J.M. and Oschkinat, H. (2000) *J. Magn. Reson.*, **143**, 411–416.
- Reif, B., van Rossum, B., Castellani, F., Rehbein, K., Diehl, A. and Oschkinat, H. (2003) *J. Am. Chem. Soc.*, **125**, 1488–1489.
- Rienstra, C.M., Hatcher, M.E., Mueller, L. J., Sun, B. Q., Fesik, S.W. and Griffin, R.G. (1998) *J. Am. Chem. Soc.*, **120**, 10602–10612.
- Sun, B.Q., Rienstra, C.M., Costa, P.R., Willamson, J.R. and Griffin, R.G. (1997) *J. Am. Chem. Soc.*, **119**, 8540–8546.
- Szeverenyi, N.M., Sullivan, M.J. and Maciel, G.E. (1982) *J. Magn. Reson.*, **47**, 462–475.
- Tycko, R., Pines, A. and Guckenheimer, J. (1985) *J. Chem. Phys.*, **83**, 2775–2802.
- Weintraub, O., Vega, S., Hoelger, Ch. and Limbach, H.H. (1994a) *J. Magn. Reson.*, **A 109**, 14–25.
- Weintraub, O., Vega, S., Hoelger, Ch. and Limbach, H.H. (1994b) *J. Magn. Reson.*, **A 110**, 12–18.
- Zaborowski, E., Zimmermann, H. and Vega, S. (1999) *J. Magn. Reson.*, **136**, 47–53.